

Yamir Moreno,^{1,2} Miguel Vázquez-Prada,¹ and Amalio F. Pacheco^{1,2}

¹*Departamento de Física Teórica, Universidad de Zaragoza, Zaragoza 50009, Spain*

²*Instituto de Biocomputación y Física de Sistemas Complejos,*

Universidad de Zaragoza, Zaragoza 50009, Spain

(Dated: May 5, 2019)

We study the phase synchronization of Kuramoto's oscillators in small parts of networks known as motifs. We first report on the system dynamics for the case of a scale-free network and show the existence of a non-trivial critical point. We compute the probability that network motifs synchronize, and find that the fitness for synchronization correlates well with motif's interconnectedness and structural complexity. Possible implications for present debates about network evolution in biological and other systems are discussed.

PACS numbers: 89.75.-k, 89.75.Fb, 05.70.Jk, 05.40.a

I. INTRODUCTION

During the last years, many scientists have scrutinized the world around us looking for regularities. One of the most recent findings is the fact that many real systems can be cast into a common topological structure, called complex networks [1]. Examples include biological [2, 3] social [4] and technological [5] systems that exhibit similar patterns of interconnections [1]. They are characterized by the existence of key elements in the network which drastically reduce the average distance between all of them, the so-called small-world property [6]. Additionally, it turns out that for a large number of real-world systems, the probability that any given element (node) of the system interacts with (is linked to) k other components, follows a power-law $P(k) \sim k^{-\gamma}$, with an exponent γ usually estimated between 2 and 3. These networks have been termed scale-free (SF) networks.

The above property was soon shown to be at the root of distinct behaviours when several dynamical processes are placed on top of SF networks. These are the cases of percolation and epidemic spreading processes, intensively studied during the last years due to their practical relevance in different applications and the availability of analytical treatments [7, 8, 9, 10, 11]. The peculiar topological properties of the underlying network for these two processes lead to the absence of any percolation or spreading threshold in the thermodynamic limit, a previously well-established result for regular and random graphs.

It is then natural to ask whether or not and to what extent the topology of complex networks influences the behaviour of other dynamical processes. In particular, for biological and other applications, it would be relevant to consider the nodes of a given network as nonlinear dynamical systems. The behaviour of an isolated generic dynamical system in the long-term limit can be described by stable fixed points, limit cycles or chaotic attractors [12]. However, we have learned in recent years that when many of such dynamical systems are coupled together, the details matter. In this way, the study of networks with both dynamical and structural complexity might shed light on a number of relevant open problems where nonlinearity and spatial complexity coexist. Dynamical complexity may manifest itself through self-organization, synchronization, the emergence of order, etc.

In this paper, we study the emergence of collective phase synchronization [13] in scale-free networks and in simple topological configurations such as triangles, squares and pentagons with a variable number of internal connections, called network motifs. To this end, we study the model proposed by Kuramoto several years ago and show how a large number of the system's constituents forms a common dynamical pattern, despite the intrinsic differences in their individual dynamics. On a theoretical level, we point out that the fitness for synchronization of network motifs correlates well with their conservation in the evolution of protein motifs [14], which might hint at new connections between graph theory, dynamics on networks and biological systems.

II. THE KURAMOTO MODEL IN SCALE-FREE NETWORKS

In order to study how topology influences collective dynamics, we assume that each network's component is an oscillator and that each interacts with the others following the Kuramoto model [15, 16]. This choice is due to the remarkable prestige achieved by synchronization as a cooperative phenomenon within nonlinear science and to the seniority, elegance and universality of this model. Specifically, each node i is considered to be a planar rotor characterized by an angular phase, θ_i , and a natural frequency ω_i . Linked nodes interact with a coupling strength λ

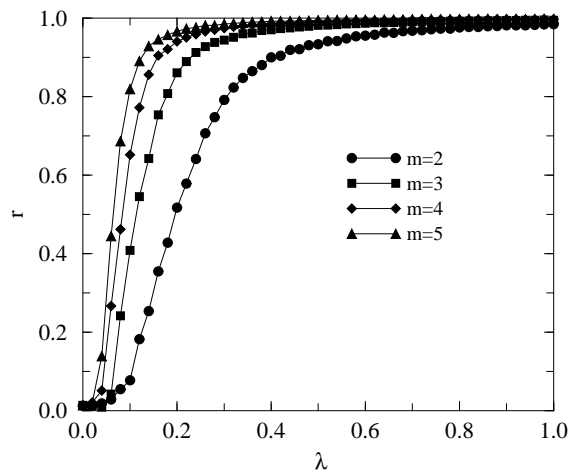


FIG. 1: Phase diagram of the Kuramoto model in random scale-free networks for several average connectivity values $\langle k \rangle = 2m$. The onset of synchronization occurs at a nonzero value of λ in all cases. Although not shown, the transition follows the mean-field behaviour exhibited by the globally coupled map. Each value of r is the result of at least 10 network realizations and 1000 iterations for $N = 10^4$ nodes.

according to

$$\frac{d\theta_i}{dt} = \omega_i + \lambda \sum_j^{k_i} \sin(\theta_j - \theta_i) \quad (1)$$

where k_i is the number of neighbors of the rotor i as given by the actual architecture of the underlying graph. For the present work, the natural frequencies and the initial values of θ_i have been randomly drawn from a uniform distribution $g(\omega)$ with mean $\omega_0 = 0$ in the interval $(-1/2, 1/2)$ and $(-\pi, \pi)$, respectively. Synchronization occurs when λ exceeds a critical value, at which clusters of frequency-locked oscillators appear. This state represents the emergence of cooperation between network's constituents.

The original Kuramoto model corresponds to the simplest case of globally coupled (all-to-all), equally weighted oscillators where the coupling strength $\lambda = K/N$ to ensure that the model is well behaved in the thermodynamic limit [15, 16]. For this model and without any interaction, $K = 0$, the oscillators follow their own dynamics as determined by their natural frequencies and thus the system is unable to synchronize. However, as K increases the population of rotors becomes more coherent and few oscillators form a small cluster of ordered (synchronized) states. If K is further increased, the synchronized pack tends to recruit more and more oscillators and eventually the system settles into a unique and totally synchronous state. The onset of synchronization occurs at a critical value of the coupling strength, $K_c = 2/\pi g(\omega_0)$. The second-order phase transition is characterized by the order parameter

$$r(t) = \left| \frac{1}{N} \sum_{j=1}^N e^{i\theta_j(t)} \right| \quad (2)$$

which behaves when both $N \rightarrow \infty$ and $t \rightarrow \infty$ as $r \sim (K - K_c)^\beta$ for $K \geq K_c$ being $\beta = 1/2$.

In order to study the dynamics of the model on top of complex heterogeneous networks, we first generated SF nets using the BA procedure [17]. In this model, starting from a set of m_0 nodes, one preferentially attaches each time step a newly introduced node to m older ones. The procedure is repeated $N - m_0$ times and a network made up of N nodes with a power law degree distribution $P(k) \sim k^{-\gamma}$ with $\gamma = 3$ and average connectivity $\langle k \rangle = 2m$ builds up. This network is a clear example of a highly heterogeneous network in that the degree distribution has unbounded fluctuations when $N \rightarrow \infty$.

We have performed extensive simulations of the model [18] through numerical integration of the equations of motion Eq. (1). In the case of random SF networks the global dynamics of the system is qualitatively the same as for the original Kuramoto model. The phase diagram of the system is shown in Fig. 1 for a network of $N = 10^4$ nodes and several values of the average connectivity $\langle k \rangle = 2m$, where r is the order parameter as given by Eq. (2). Starting from small values of the coupling strength, the interactions do not overcome the tendency of each rotor to oscillate according to its individual dynamics. In this state, the behaviour of the system is completely incoherent and no synchronization

is achieved. This picture persists until a certain critical value λ_c is crossed. At this point some elements lock their phase and a cluster of synchronized nodes comes up. This constitutes the onset of synchronization. Beyond this value, there are several groups or clusters within which the nodes are either synchronized and locked in phase or still governed by their intrinsic dynamics and thus in an asynchronous state. The first groups add to r and it departs from zero as λ is increased beyond λ_c . Finally, after further increasing the value of λ , more and more nodes cluster around the mean phase and the system eventually settles into a completely synchronized state where $r \approx 1$.

On the other hand, Fig. 1 also provides evidence that the critical point at which synchronization is attained in these SF networks is not zero [18]. This is more clearly appreciated if one eliminates the dependency observed in the figure of the parameter r on the average connectivity of the network $\langle k \rangle$. If in Eq. (1) the term λ is substituted by $\lambda/\langle k \rangle$, the $\langle k \rangle$ -dependency is avoided and all curves in Fig. 1 collapse into a single one, showing a critical coupling strength $\lambda_c = 0.25(3)$ signaling that even for large values of the average connectivity, λ_c is not equal to zero. Additionally, finite-size scaling analysis [18] shows that the transition remains of the second-order type as for the case of fully connected networks.

III. SYNCHRONIZATION OF NETWORK MOTIFS

Let's now turn our attention to small geometrical structures known as motifs [19, 20, 21] instead of looking at the whole network. These structures can be defined as graph components which are observed in a given network more frequently than in a completely random graph with identical $P(k)$. Triangles and rectangular loops are among these graph components, also known as cycles. They are important because they express the degree of redundancy and multiplicity of paths among nodes in the topology of the network and reveal the existence of hierarchical levels. Hence, the extension of the study of synchronization phenomena to motifs is also relevant.

We have computed for all motifs up to $N = 4$ nodes the probability, P_{sync} , that synchronization occurs. This probability is an increasing function of λ , and is calculated for each λ by randomly drawing the values of the natural frequencies ω_i from a uniform distribution in the interval $(-1/2, 1/2)$. Starting from $\lambda = 0$, one averages, for every λ , over many realizations of ω_i and computes the relative number of simulations where synchronization is accomplished, P_{sync} . We define λ^* , which varies from motif to motif, as the value of λ beyond which $P_{sync} \geq \frac{1}{2}$. The lower λ^* is for a motif, the better it synchronizes. In Fig. 2, we have represented P_{sync} as a function of λ for several motifs.

The simplest case of the dimer (#1 in the Table) can be deduced analytically. Using the same notation as in Eq. (1), here we have:

$$\frac{d\theta_1}{dt} = \omega_1 + \lambda \sin(\theta_2 - \theta_1), \quad \frac{d\theta_2}{dt} = \omega_2 + \lambda \sin(\theta_1 - \theta_2). \quad (3)$$

To solve these equations, we introduce the new variables,

$$f = \theta_2 - \theta_1, \quad \kappa = \omega_2 - \omega_1, \quad c = \frac{2\lambda}{\kappa}. \quad (4)$$

Thus, f is the phase difference between the rotors, κ is the difference in the natural frequencies and c is a dimensionless constant equal to twice the ratio λ/κ . From Eq. (3) we obtain,

$$\frac{df}{\kappa(1 - c \sin f)} = dt. \quad (5)$$

The integration of Eq. (5) leads to three solutions depending on the value of c . The three distinct results of the integral in Eq. (5) indicate a different functional behaviour of the system when $c < 1$, $c = 1$, and when $c > 1$. In fact, $c = 1$ is the critical point. In consequence, from the definition of c in Eq. (4), the critical coupling of this system corresponds to

$$\lambda^* = \frac{\kappa}{2} = (\omega_2 - \omega_1)/2. \quad (6)$$

Recalling that the ω s are drawn from a uniform probability distribution in the interval $(-1/2, 1/2)$ with a mean equal to zero, i.e., $\omega_1 = -\omega_2 = \omega$, we have that the synchronization condition reduces to $\lambda \geq \omega$. The probability P_{sync} is then equal to $P_{sync} = \frac{\lambda}{1/2} = 2\lambda$, for $\lambda < \frac{1}{2}$, and $P_{sync} = 1$ for $\lambda \geq \frac{1}{2}$. Thus, for the dimer we have $\lambda^* = \frac{1}{4}$. For

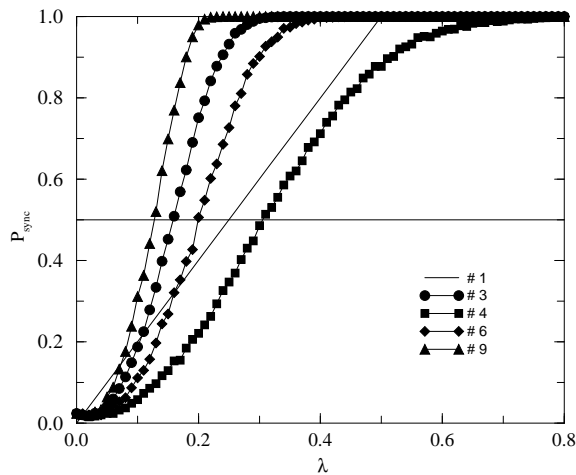


FIG. 2: Probability of synchronization for five topological motifs. Configurations are according to Table I. Each value of P_{sync} is the result of 1000 iterations over the distribution of ω_i for each value of λ . The horizontal line marks the threshold of P_{sync} for the computation of λ^* . See the text for further details.

the other motifs, P_{sync} has been calculated numerically by means of a 4th-order Runge-Kutta method. The results are summarized in Fig. 2 for several motifs (see also Table I below).

From Fig. 2, one realizes that for a fixed motif's size, the way in which connections are established determines the synchronization threshold of that motif configuration. For instance, configurations 4, 6, and 9 correspond to motifs made up of four oscillators with a variable number of connections among them. However, their λ^* are quite different. This indicates that the details of the local and internal connections matter. In particular, we observe that the higher the interconnection between motif's constituents, the lower λ^* .

IV. DISCUSSIONS AND CONCLUSIONS

We now show how the present study may provide useful hints to a better understanding of several experimental observations in biological systems. Recent advances in network analysis and modeling have provided a promising approach to understanding basic biological organization [22, 23]. In this context, quantitative evidence has been recently reported [14] that in *Saccharomyces cerevisiae*, the proteins organized in definite cohesive patterns of interaction, and these patterns themselves, are conserved in the evolution across species in a substantially higher degree than those that do not participate in such specific motifs. A second finding [14] is that the conservation of proteins in distinct topological motifs correlates with their interconnectedness.

These observations take place in the context of activities occurring within a living cell and which no doubt, are of extreme complexity. Non-linear dynamics prevails at this level of organization, where units that interact according to simple rules can generate unexpected complex patterns [12]. On a theoretical level, one may hypothesize that the observed persistence across evolution is due to some mechanism aimed at optimizing the cooperation between neighboring nodes. A first approach would then be to see if the same structures favor the synchronization as a cooperative phenomenon.

Table 1 summarizes the results found in [14] and the values of λ^* for the Kuramoto's model in the same motifs. It is surprising the existence of a possible correlation between conservation and fitness for synchronization of network motifs. Namely, the lower λ^* , the higher the natural conservation rate. From Table I, one observes that: *i*) $\lambda_1^* < \lambda_2^* < \lambda_5^*$, for the chain-like motifs; *ii*) $\lambda_5^* > \lambda_7^* > \lambda_8^* > \lambda_9^*$, for motifs ordered in increasing degree of complexity, i.e., when one can go from the lower configuration (5) to next one by adding a new link arbitrarily; and *iii*) $\lambda_5^* > \lambda_6^* > \lambda_8^* > \lambda_9^*$, when interconnectedness between motif constituents increases. This may indicate that motifs displaying an improved fitness to develop cooperative activities are preserved across evolution with a higher probability.

The results here obtained for topological motifs may be seen on a more general basis concerning the architecture of real biological and social networks. It is known that for most of these networks, the probability of finding cycles (motifs) in their structure is higher than that expected from a completely random graph with the same connectivity distribution. For social and biological networks, friendship or business relationships and natural selection seem to be at the origin of such cycles. From this perspective, one may assume that these networks have been shaped during their evolution by some kind of optimization mechanism that improves on a local level their ability to develop cooperation.

#	Motif	λ^*	NCR (%)
1		0.25	13.67
2		0.28	4.99
3		0.16	20.51
4		0.31	0.73
5		0.32	2.64
6		0.20	6.71
7		0.22	7.67
8		0.18	18.68
9		0.14	32.53

TABLE I: The third column gives the value of the coupling strength beyond which the motif synchronizes with probability $P_{sync} \geq \frac{1}{2}$. Natural conservation rates (NCR) reported in the table are taken from [14]. The values reported are sorted in such a way that for a fixed N , the NCR values are in increasing order. Although not shown due to the lack of NCR values, our conclusions hold for five-node and higher motifs. In particular, it is straightforward to conclude from the mean-field description of the Kuramoto model (all-to-all architecture) that as N increases, the synchronization threshold decreases.

If a new link is created and afterwards it reveals as not beneficial, then it is removed at later times.

In summary, we have studied the synchronization of Kuramoto's phase coupled oscillators for the cases of scale-free networks and motifs. The results obtained indicate that the architecture of random SF networks allows synchronization at a small value of the coupling strength λ . Additionally, motifs with high interconnectedness show the lower synchronization thresholds. Moreover, the results presented here for the Kuramoto's model hold for other non-linear dynamical systems, including chaotic oscillators [24]. Our results then lead to a twofold conclusion. On one hand, they suggest that non-linear mechanisms may be key ingredients for the understanding of the evolution of networks at a local scale. On the other hand, as recently unraveled for protein and other biological networks, the real topology of the systems under analysis is worth taking into account [25]. Finally, we point out that the kind of models studied here together with the spatial complexity of the underlying net is relevant for cell biology. A recent example can be found in the discovery that an ultradian clock (oscillator) shapes genome expression in the yeast *Saccharomyces cerevisiae* [26].

Acknowledgments

Y. M. acknowledges financial support from a BIFI research grant. This work has been partially supported by the Spanish DGICYT project BFM2002-01798.

-
- [1] S. H. Strogatz, *Nature (London)* **410**, 268 (2001).
 - [2] H. Jeong, S. P. Mason, A.-L. Barabási, and Z. N. Oltvai, *Nature (London)* **411**, 41 (2001).
 - [3] R. V. Solé, and J. M. Montoya, *Proc. R. Soc. London B* **268**, 2039 (2001).
 - [4] M. E. J. Newman, *Proc. Natl. Acad. Sci. U.S.A.* **98**, 404 (2001).
 - [5] A. Vázquez, R. Pastor-Satorras, and A. Vespignani, *Phys. Rev. E* **65**, 066130 (2002).
 - [6] D. J. Watts and H. S. Strogatz, *Nature* **393**, 440 (1998).
 - [7] D. S. Callaway, M. E. J. Newman, S. H. Strogatz, and D. J. Watts, *Phys. Rev. Lett.* **85**, 5468 (2000).
 - [8] R. Pastor-Satorras, and A. Vespignani, *Phys. Rev. Lett.* **86**, 3200 (2001).
 - [9] Y. Moreno, R. Pastor-Satorras, and A. Vespignani, *Eur. Phys. J. B* **26**, 521 (2002).
 - [10] A. Vázquez, and Y. Moreno, *Phys. Rev. E* **67**, 015101(R) (2003).
 - [11] Y. Moreno, J. B. Gómez, and A. F. Pacheco, *Phys. Rev. E* **68**, 035103(R) (2003).
 - [12] S. H. Strogatz, *Nonlinear dynamics and chaos* (Reading, MA: Perseus Books, Cambridge MA, 1994).

- [13] A. Pikovsky, M. Rosenblum, and J. Kurths, *Synchronization: A Universal Concept in Nonlinear Science* (Cambridge Univ. Press, Cambridge, 2001).
- [14] S. Wuchty, Z. N. Oltvai, and A.-L. Barabási, *Nat. Genet.* 35, 176-179 (2003).
- [15] Y. Kuramoto, *Chemical Oscillations, Waves, and Turbulence* (Springer, Berlin, 1984).
- [16] S. H. Strogatz, *Physica D* **143**, 1 (2000).
- [17] A.-L. Barabási, and R. Albert, *Science* **286**, 509 (1999); A.-L. Barabási, R. Albert, and H. Jeong, *Physica A* **272**, 173 (1999).
- [18] Y. Moreno, and A. F. Pacheco, unpublished, preprint cond-mat/0401266 (2004).
- [19] S. Itzkovitz, R. Milo, N. Kashtan, G. Ziv and U. Alon, *Phys.Rev. E* **68**, 026127. (2003).
- [20] R. Milo, S. Shen-Orr, S. Itzkovitz, N. Kashtan, D. Chklovskii and U. Alon, *Science* **298**, 824 (2002).
- [21] G. Bianconi and A. Capocci, *Phys. Rev. Lett.* **90**, 078701 (2003).
- [22] J. Hasty, D. McMillen, and J. J. Collins, *Nature* 420, 224-230 (2002).
- [23] H. Kitano, *Science* 295, 1662 (2002).
- [24] Barahona, M. and Pecora, L.M. *Phys. Rev. Lett.* 89, 054101 (2002).
- [25] A. Vespignani, *Nat. Genet.* 35, 118 (2003).
- [26] R. R. Klevecz, J. Bolen, G. Forrest, and D. B. Murray, *Proc. Natl. Acad. Sci. USA* **101**, 1200 (2004).